

Tools and Methods for the Registration of Remotely Sensed Data

Jacqueline Le Moigne
(NASA Goddard Space Flight Center)

Extracted from Tutorial by A.A. Goshtasby and J. Le Moigne,
“HD-5: Tools and Methods for the Registration and Fusion of Remotely Sensed Data,”
2010 IEEE International Geoscience and Remote Sensing Symposium, IGARSS’10, Hawaii, July 25, 2010

Introduction and background

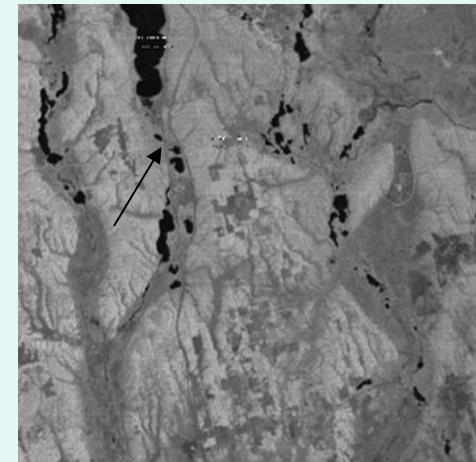
A digital image: An array of scalars or vectors.

Scalar: *Reflectance, temperature, range*

Vector: *RGB, multispectral, hyperspectral*

```
126 132 124 120 126 124 116 132 126 106 100 104 122 130 120 108
130 136 124 124 124 126 126 132 128 114 104 104 126 136 122 112
130 136 132 126 104 108 122 122 126 120 108 112 128 130 118 112
132 132 128 84 42 40 54 82 112 118 108 118 136 134 114 114
130 132 132 70 4 0 10 32 64 102 116 116 134 130 114 114
128 134 136 102 44 20 16 10 22 78 116 108 124 120 116 114
132 132 136 128 102 60 20 10 22 60 108 108 120 120 112 110
128 126 124 122 124 110 78 48 34 50 100 98 90 118 122 116
122 126 120 114 122 132 128 108 90 86 106 100 84 114 120 114
126 134 130 124 124 124 124 136 140 134 120 110 110 110 106 102
138 138 136 128 124 124 132 130 132 136 124 106 114 114 108 104
```

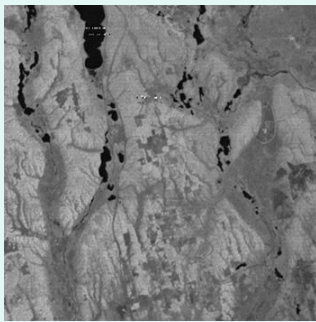
A digital image



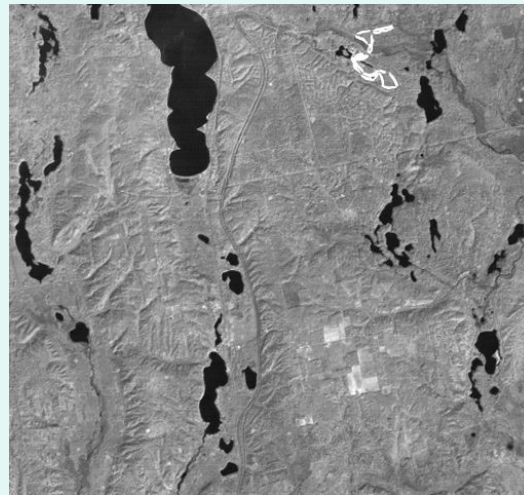
Landsat MSS image,
courtesy of NASA

Image registration and image fusion

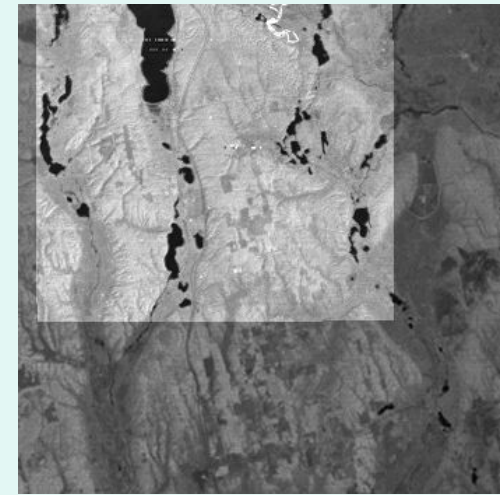
Image registration is the process of spatially aligning two or more images of a scene. This spatial alignment is needed to fuse information in the images.



Landsat MSS



Landsat TM

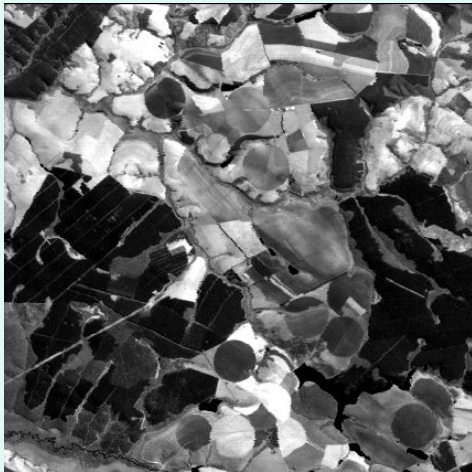


Registered MSS & TM

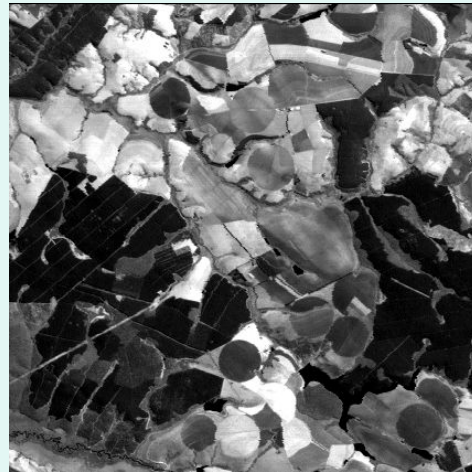
Data courtesy of NASA

Applications of image registration and image fusion

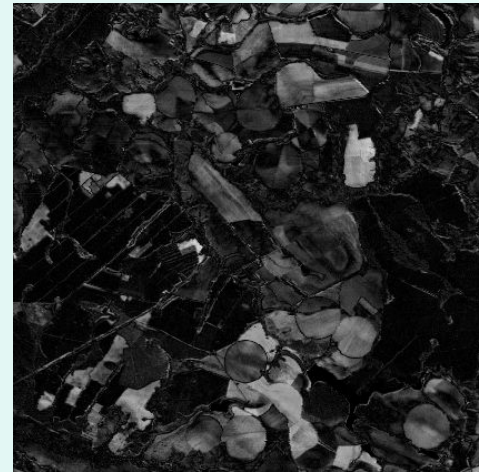
Change detection



Landsat 1



Landsat 2



Change image

Data courtesy of NASA

Fusion of multimodal data



Fused image

Data courtesy of NASA



Landsat TM bands 1 & 7

Image mosaicking



Mosaicked image



Two aerial images of Honolulu, HI.

Need for Fast and Accurate Image Registration

- Earth Science studies, e.g.:
 - Predicting crop yield
 - Evaluating climate change over multiple scales
 - Locating arable land and water resources
 - Monitoring pollution
 - Understanding the impact of human activity on major Earth ecosystems, etc.
- Global and repetitive measurements from a wide variety of satellite remote sensing systems

Landsat ETM and IKONOS Registration US, Virginia Coast

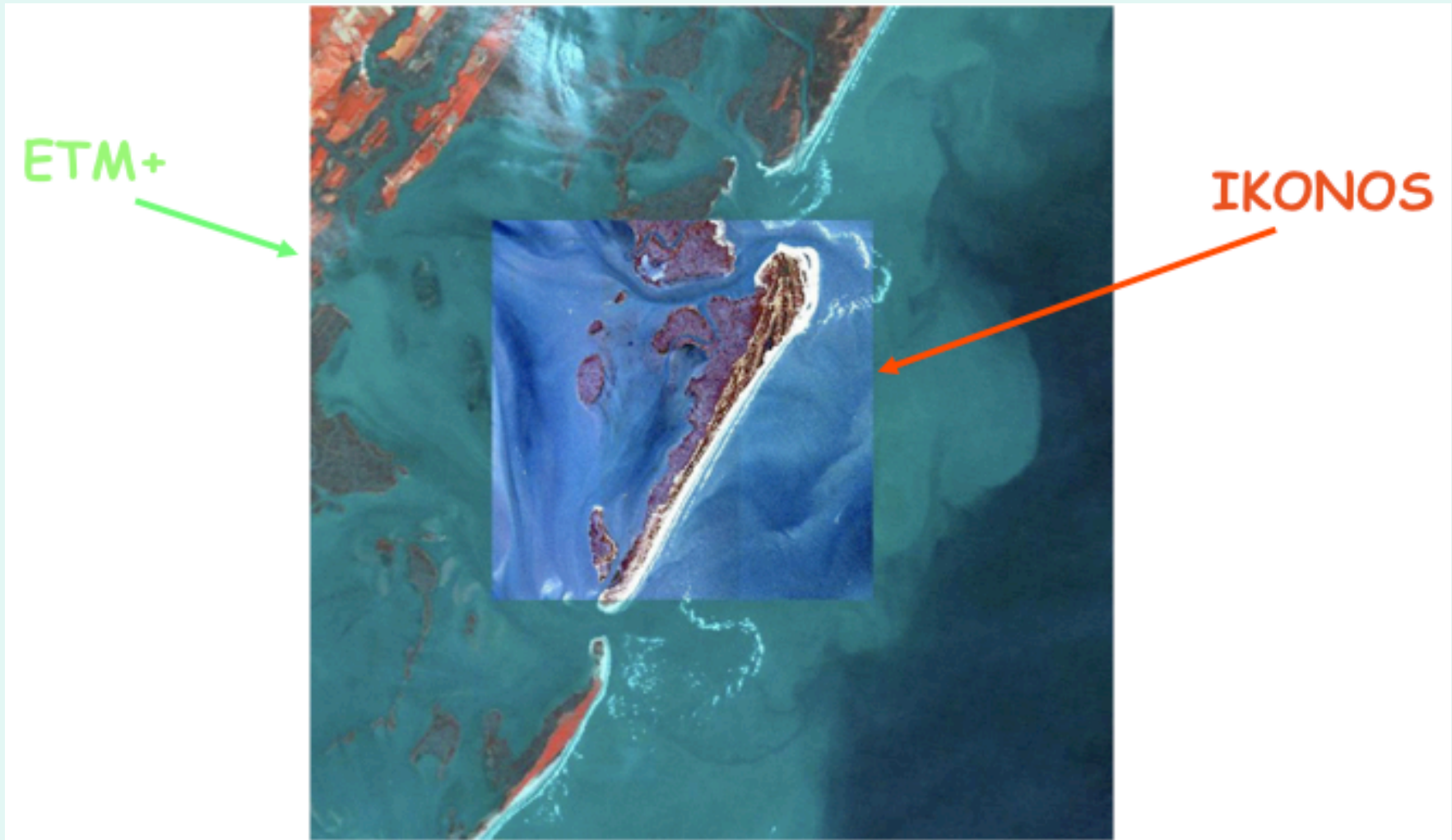
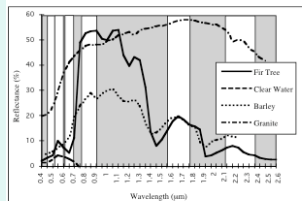
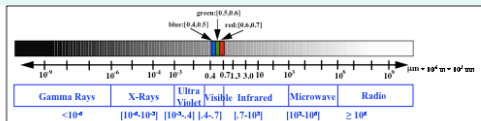
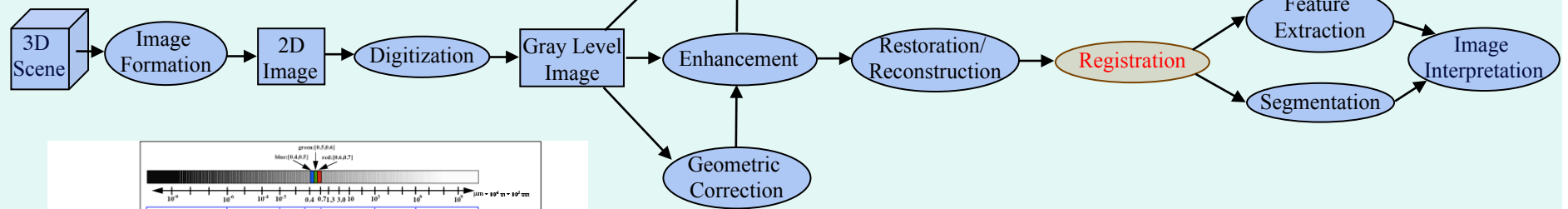
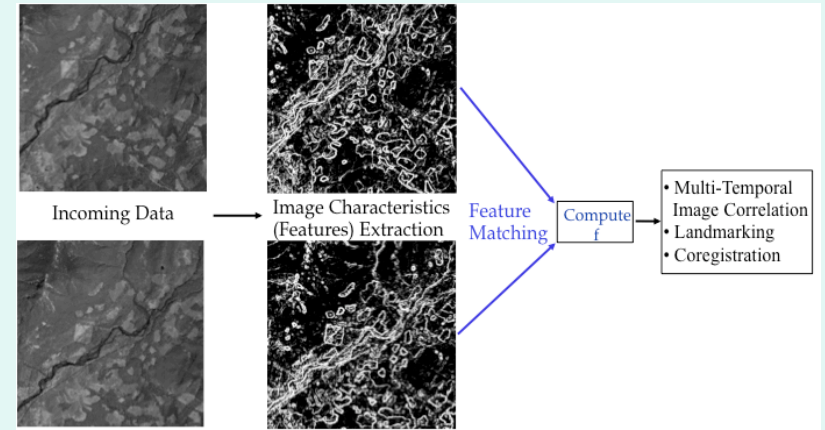
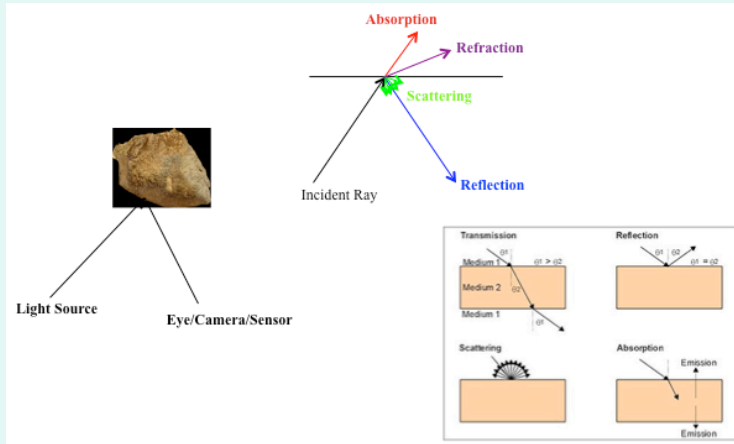


Image Processing Framework for Remotely Sensed Data



Examples of Spectral Response Patterns for 4 Different Types of Features - Fir Tree, Clear Water, Barley, Granite - White Areas Show the Portions of the Spectrum Corresponding to the 7 Channels of Landsat-Thematic Mapper (TM)

Signal to Noise at Wavelength λ :

$$(S/N)_\lambda = D_\lambda \beta^2 (H/V)^2 \Delta\lambda L_\lambda$$

Where

- D_λ : detectivity (measures detector performance quality)
- β : instantaneous field of view
- H : flying height of the spacecraft
- V : velocity of the spacecraft
- $\Delta\lambda$: spectral bandwidth of the channel (spectral resolution)
- L_λ : spectral radiance of ground feature

=> Tradeoff between spatial and spectral resolutions. e.g.:
To maintain the same SNR while improving spatial resolution by a factor of 4 (i.e., decreasing β by a factor of 2), we must degrade the spectral resolution by a factor of 4 (i.e., increase $\Delta\lambda$ by a factor of 4)

The role of Image Registration in the Processing of Remotely Sensed Data

- Essential for spatial and radiometric calibration of multitemporal measurements for creating long-term phenomenon tracking data
- Used for accurate change detection:
 - (Townshead et al, 1992) and (Dai & Khorram, 1998): small error in registration may have a large impact on global change measurements accuracy
 - e.g., 1 pixel misregistration error => 50% error in NDVI^{*} computation (using 250m MODIS data)
- Basis for extrapolating data throughout several scales for multi-scale phenomena (distinguish between natural and human-induced)

* Normalized Difference Vegetation Index

Classifying Image Registration Utilization

- *Multimodal registration*, for integrating complementary information from multiple sensors
- *Multitemporal registration*, for change detection and Earth resource surveying
- *Viewpoint registration*, for landmark navigation, formation flying (sensor web) and planet exploration
- *Template registration*, for content-based searching or map updating

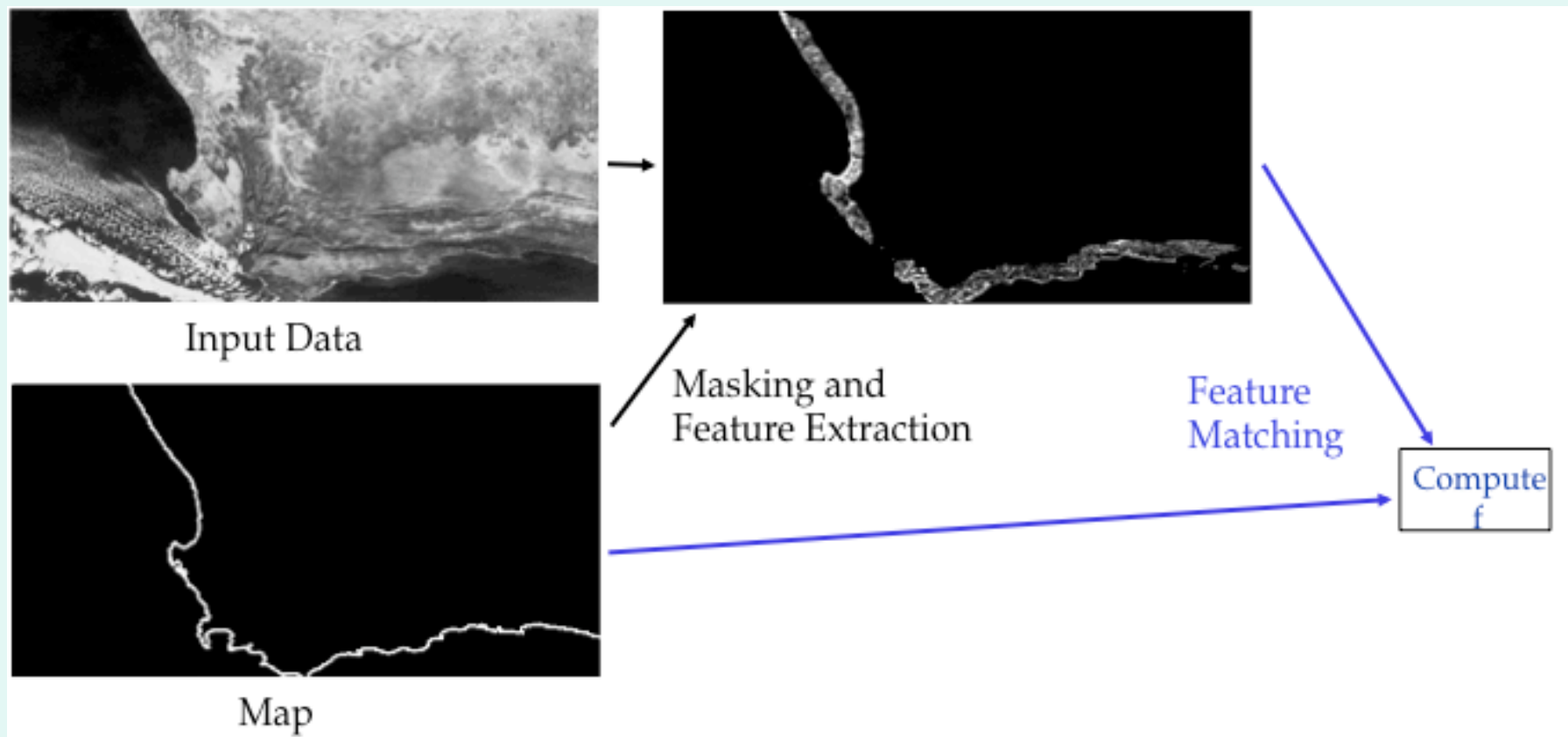
Image Registration Requirements

- *High Accuracy*: Goal of sub-pixel accuracy
- *Consistency*: Robustness to recurring use
- *Speed and High-Level of Autonomy*: Needed for
 - Large amounts of data
 - Near- or Near-real time applications (e.g., disaster management)

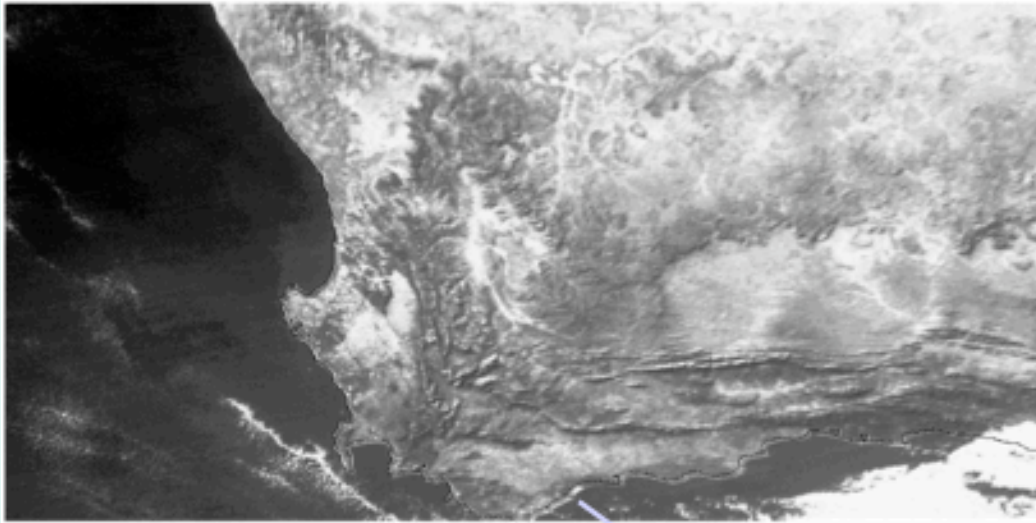
Systematic and Precision Corrections

- **Navigation or Model-Based Systematic Correction**
 - Orbital, attitude, platform/sensor geometric relationship, sensor characteristics, Earth model, etc.
- **Image Registration or Feature-Based Precision Correction**
 - Navigation within a few pixels accuracy
 - Image registration using selected features (or Control Points) to refine geo-location accuracy
- **Two approaches**
 1. Image registration as post-processing
 2. Navigation and image registration in a closed loop

Systematic and Precision Corrections AVHRR Example

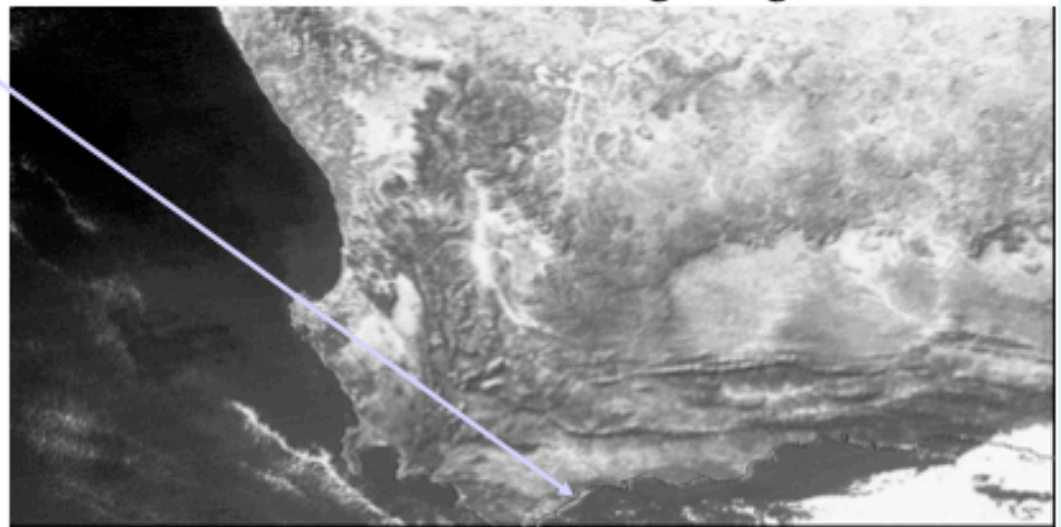


Systematic and Precision Corrections AVHRR Example (cont.)



After Navigation and
Before Image Registration

After Image Registration



Challenges in Registration of Remotely Sensed Data

- Image registration developed in other domains (medical, military, etc.) not always applicable
 - Variety in the types of sensor data and the conditions of data acquisition
 - Size of the data
 - Lack of a known image model
 - Lack of well-distributed “fiducial point” resulting in the difficulty to validate image registration methods in the remote sensing domain
 - » use synthetic data, “ground truth”, finer resolution data and “circular” registrations

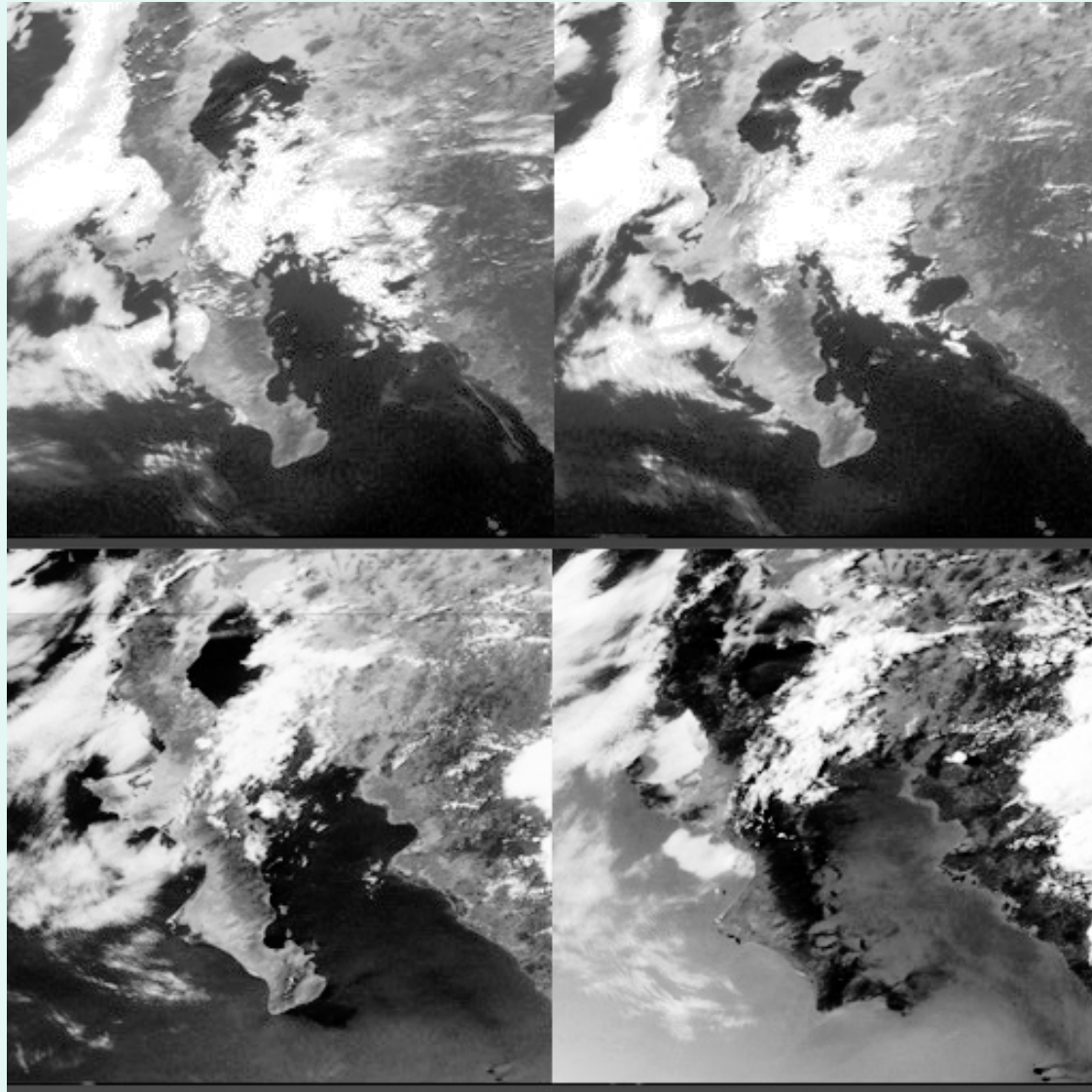
Other Challenges Facing Image Registration In the Remote Sensing Domain

- Navigation error
 - Historical satellites (e.g., Landsat-5 compared to Landsat-7)
 - Following a maneuver (e.g., star tracking)
 - Need for sub-pixel accuracy
- Atmospheric and cloud interactions
- Multitemporal effects
- Terrain/relief effect
- Multisensor data with different spatial and spectral resolutions

Atmospheric and Cloud Interactions

Baja Peninsula, California; 4 different times of the day (GOES-8)

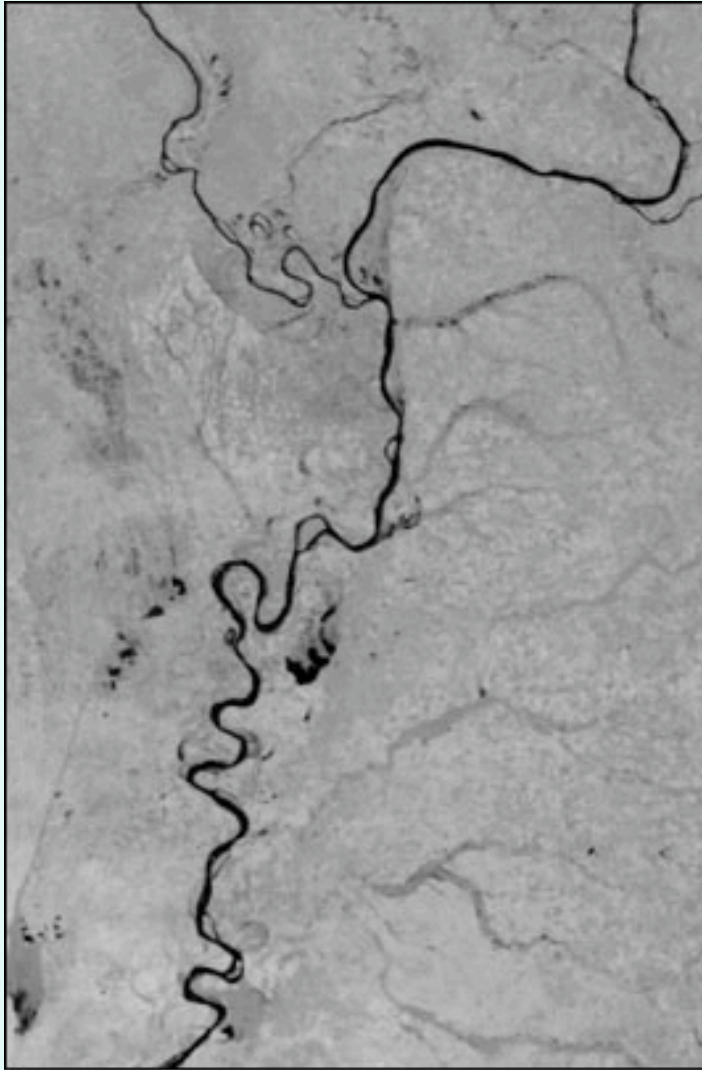
(Reproduced from Le Moigne & Eastman, 2005)



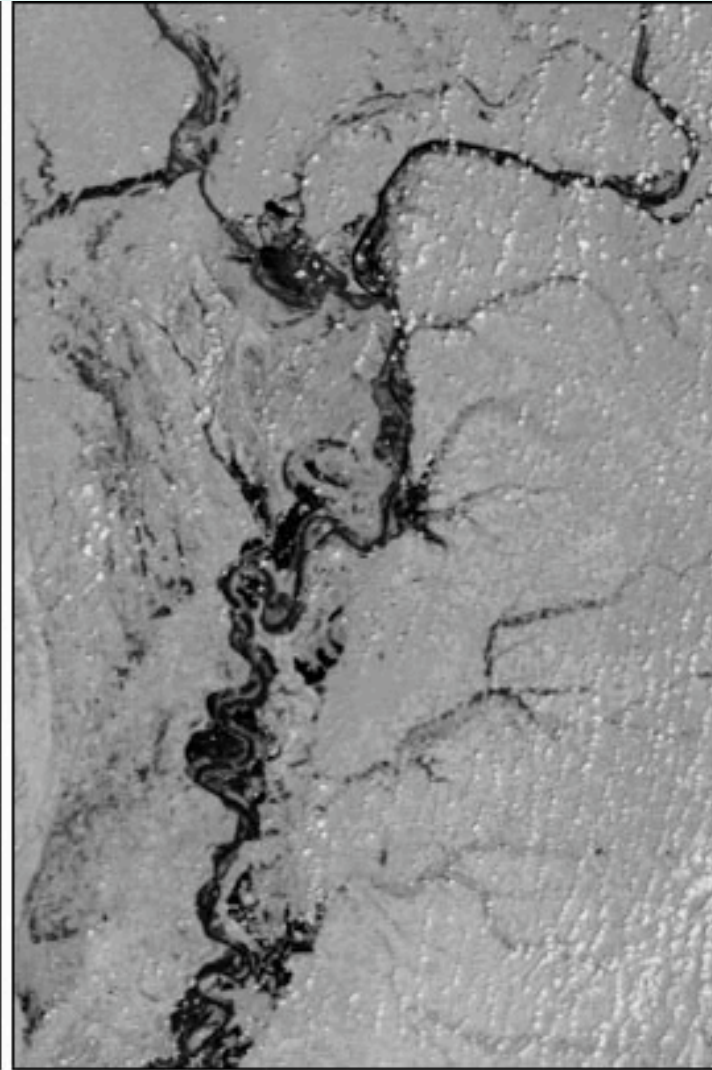
Multitemporal Effects

Mississippi and Ohio Rivers before & after Flood of Spring 2002 (Terra/MODIS)

(Reproduced from Le Moigne & Eastman, 2005)



April 25, 2002

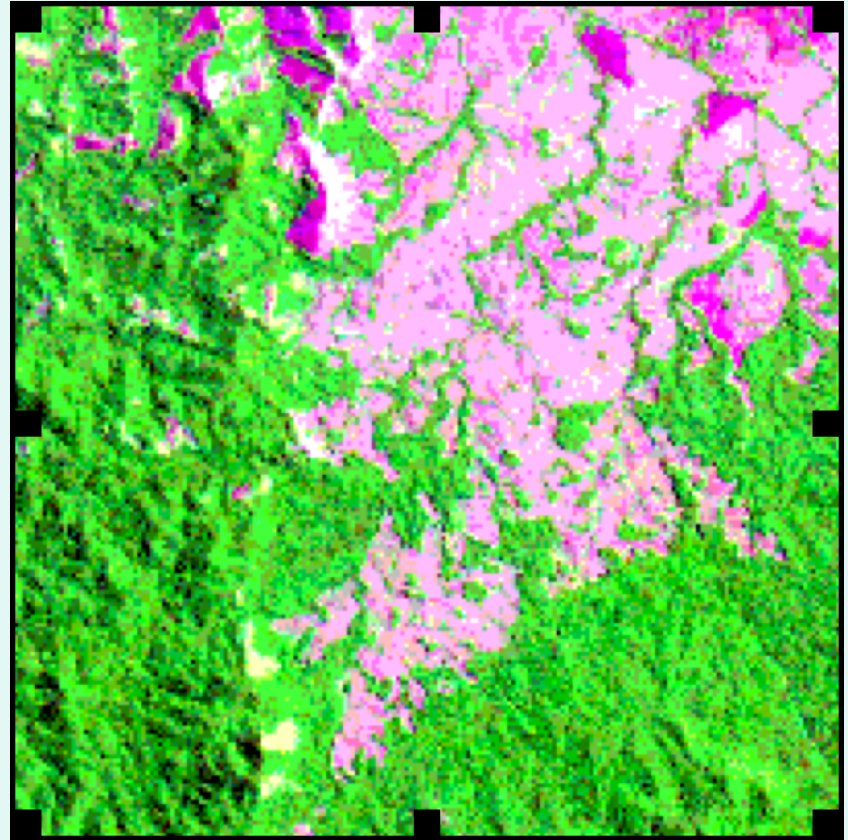
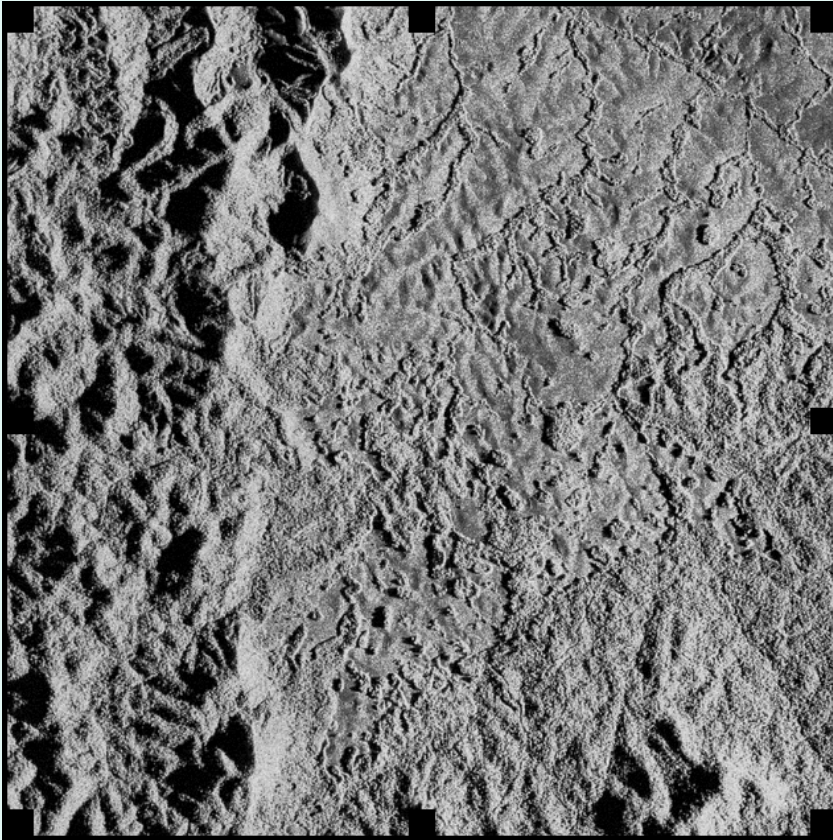


May 18, 2002

Relief Effect

SAR and Landsat-TM Data of Lopé Area, Gabon, Africa

(Reproduced from Le Moigne et al., 2001)



Precision Correction in Operational Systems

- Operational Environment

- Platform/sensor models integrated
- Historical data available for statistics/modeling
- Robustness and consistency over time is a requirement

- Operational Needs

- Systematic correction (close to 1 pixel) using navigation model
- Precision correction (less than 1 pixel) used to:
 - Check navigation model and ephemeris data
 - Perform band to band geometric calibration
 - Perform radiometric calibration of new sensor (relative to old one)

- General Characteristics

- Use database of Ground Control Points (GCP) or Chips
- Normalized Cross-Correlation (NCC) is the most common similarity measure
- Digital Elevation Model (DEM) is rarely integrated in the registration process
- Cloud masking usually integrated
- Errors in the [0.15-0.5] range

Precision Correction in Operational Systems

Some Examples - Highlights

- **AVHRR:** AUTONAV algorithm computes attitude corrections using Maximum Cross-Correlation (MCC) method between sequential images
- **GOES/METEOSAT:** CPs and NOAA Shoreline database (GSHHS) used to match edges extracted from meteorological images
- **LANDSAT:** CP image chips (1m orthorectified) using Gaussian pyramid, automatic Moravec window extraction and NCC or Mutual Information
- **MISR:** Database of 120 GCPs (each a collection of nine geolocated image patches of a well-defined and easily identifiable ground features, from Landsat, terrain-corrected, data) & ray casting simulation software
- **MODIS:** Biases and trends in the sensor orientation determined from automated control point (CP) matching and removed by updating models of the spacecraft and instrument orientation; finer CGPs from Landsat TM and ETM aggregated using PSFs and correlated with NCC
- **SEAWIFS:** Reference catalog of islands GCPs and matching using spectral classification and clustering of data, “nearest neighbor” and pattern matching techniques
- **SPOT:** Reference3D™ using DEM ortho-rectified simulated reference image in focal plane geometry, matching of input image to simulated using NCC and resampling into a cartographic reference frame
- **VEGETATION:** Database of CPs from SPOT for VEGETATION1 and VEGETATION1 for VEGETATION2; Matching by NCC

Image Registration at NASA GSFC

- **Operational Environment**

- Platform/sensor models integrated
- Historical data available for statistics/modeling
- Robustness and consistency over time is a requirement

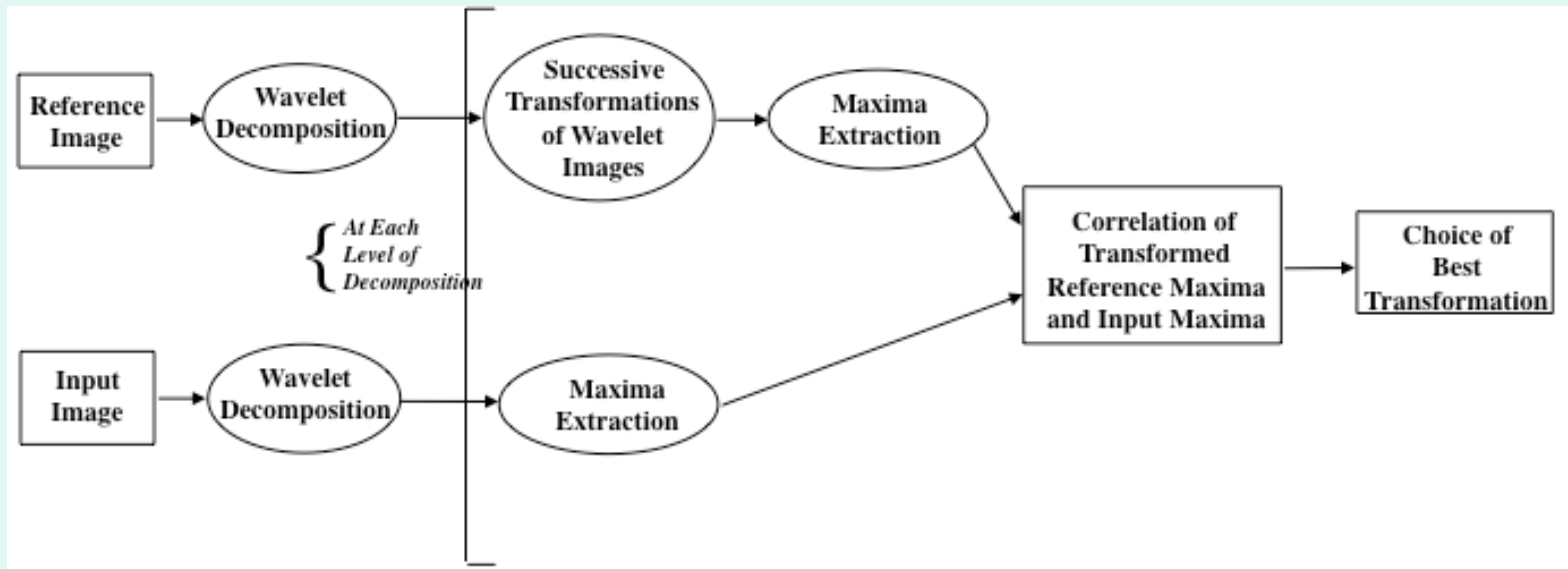
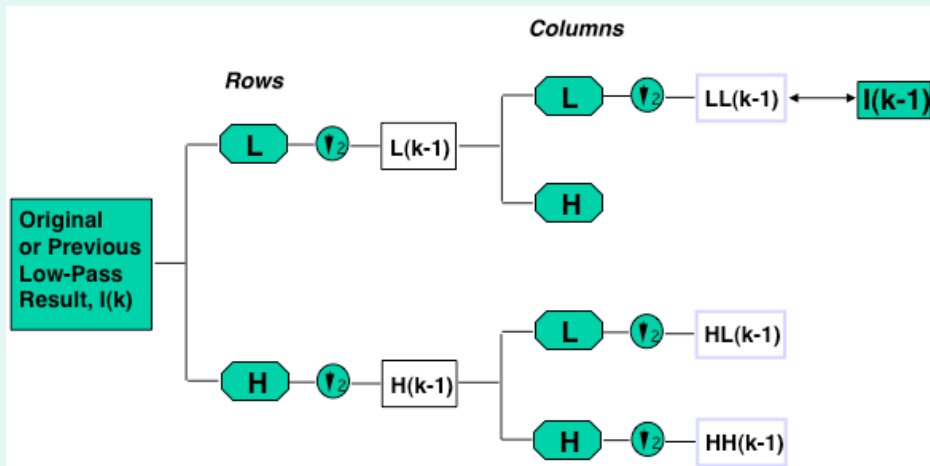
- **Operational Needs**

- Systematic correction (close to 1 pixel) using navigation model
- Precision correction (less than 1 pixel) used to:
 - Check navigation model and ephemeris data
 - Perform band to band geometric calibration
 - Perform radiometric calibration of new sensor (relative to old one)

- **General Characteristics**

- Use database of Ground Control Points (GCP) or Chips
- Normalized Cross-Correlation (NCC) is the most common similarity measure
- Digital Elevation Model (DEM) is rarely integrated in the registration process
- Cloud masking usually integrated
- Errors in the [0.15-0.5] range

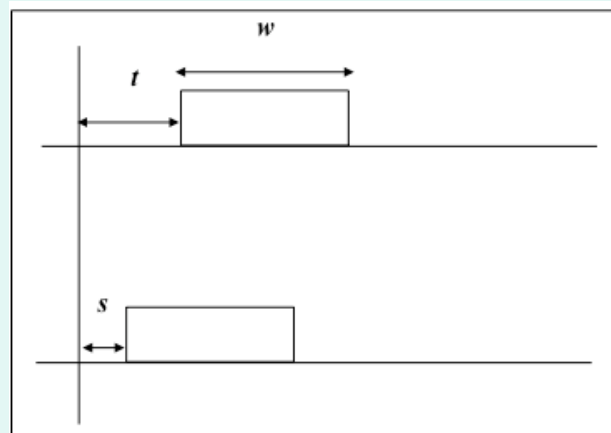
Orthogonal Wavelet Image Registration



Orthogonal Wavelet Image Registration

Rotation and Translation Invariance Issues

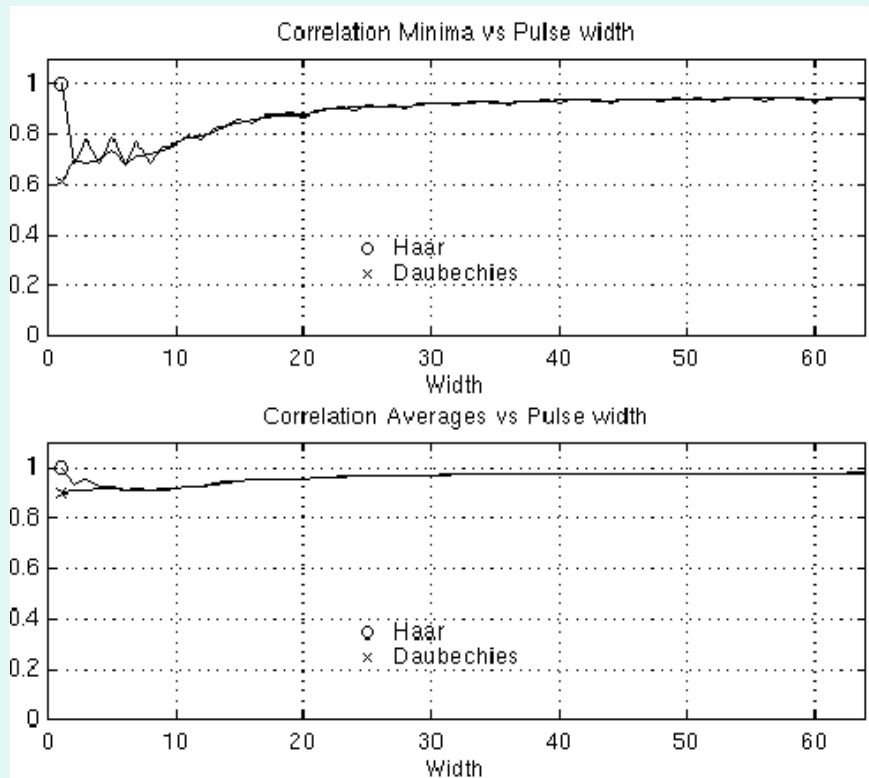
- Nyquist criterion, sample signal at least twice frequency of highest frequency component
 - in og wavelets, signal changes within or across subbands with subsampling
- Study for Shift Sensitivity (Stone et al, 1999):
 - low-pass subband relatively insensitive to translation, if features are twice the size of wavelet filters
 - high-pass subband more sensitive but can still be used.



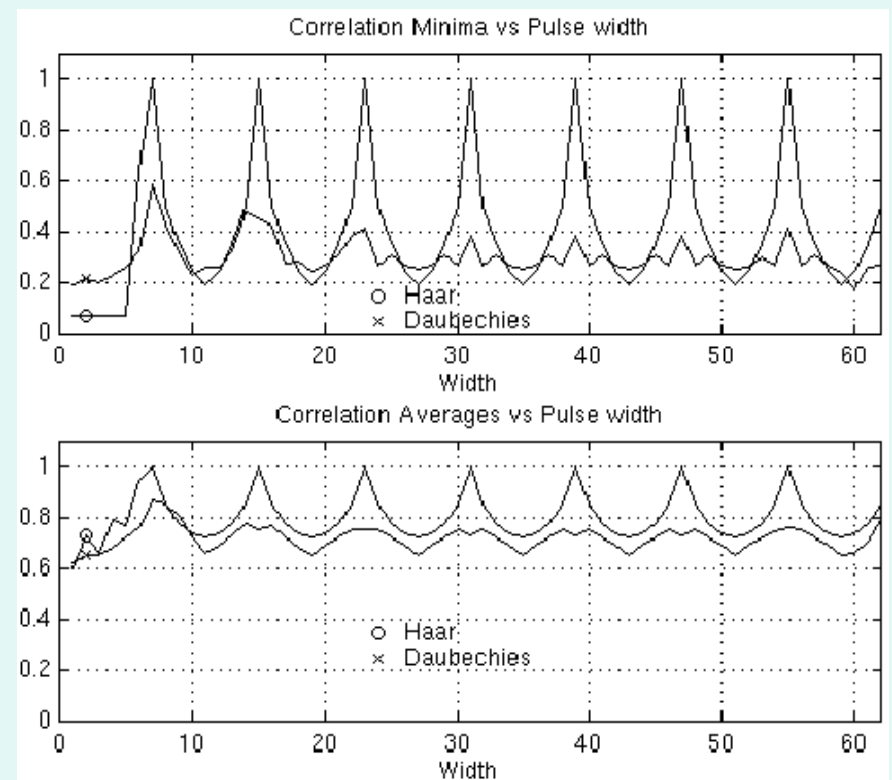
Correlate Wavelets of Two Pulses

Orthogonal Wavelet Image Registration

Rotation and Translation Invariance Issues (cont.)



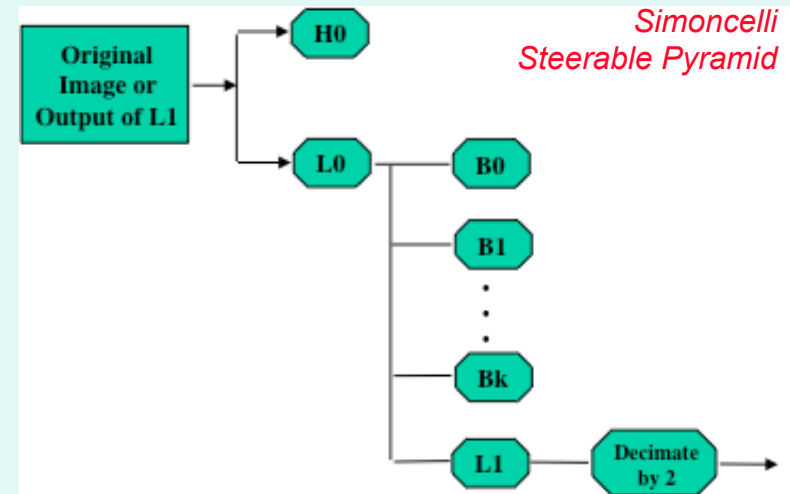
Translation Sensitivity Low-Pass Level 3



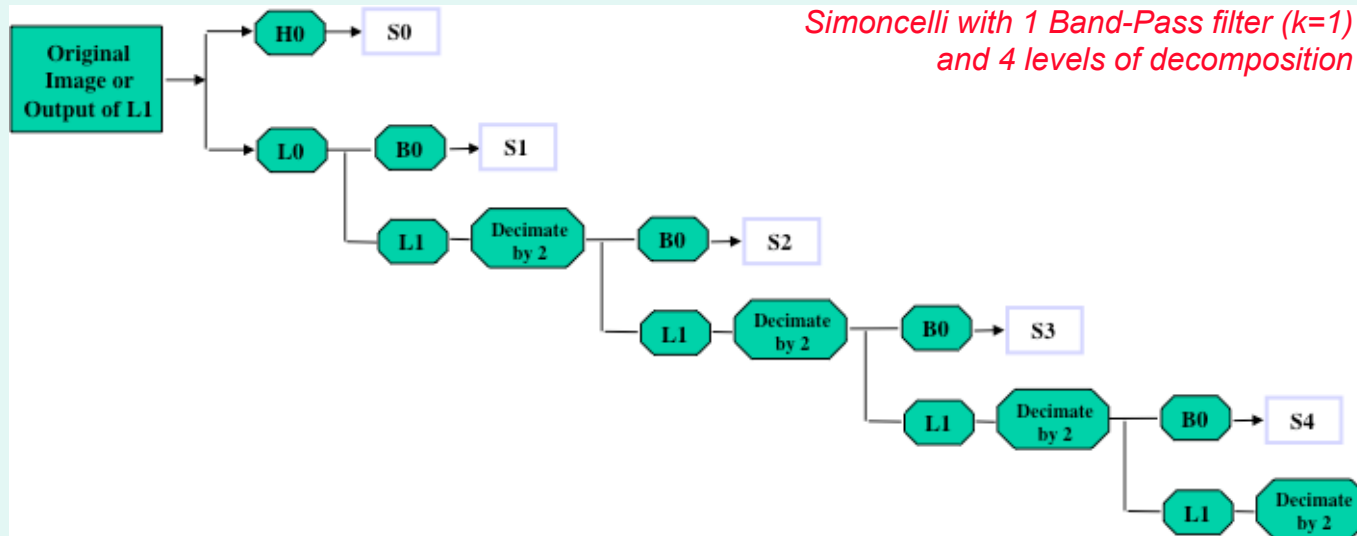
Translation Sensitivity High-Pass Level 3

Rotation- and Translation-Invariant Pyramids

- Simoncelli:
 - Relax critical sampling condition of wavelet transforms
 - Overcomplete representation by $4k/3$ (k : number of band-pass filters)
- Splines:
 - Recursive anti-aliasing prefiltering followed by a decimation of 2
 - Only low-pass bands



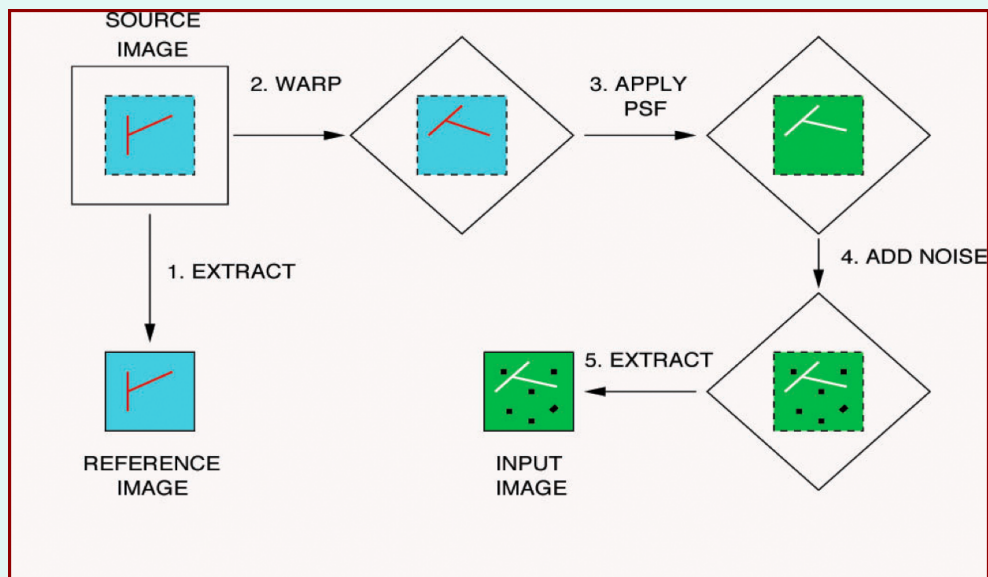
Simoncelli Steerable Pyramid



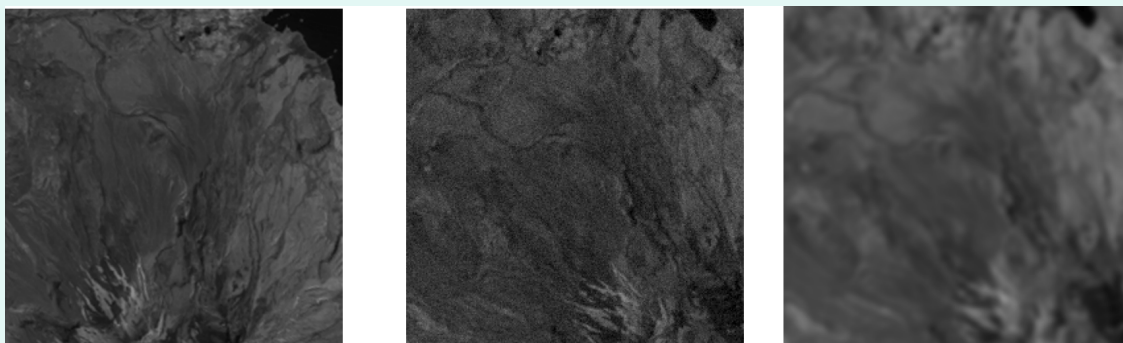
Simoncelli with 1 Band-Pass filter ($k=1$) and 4 levels of decomposition

Comparative Studies Using Synthetic Data

(Reproduced from Zavorin & Le Moigne, 2005)



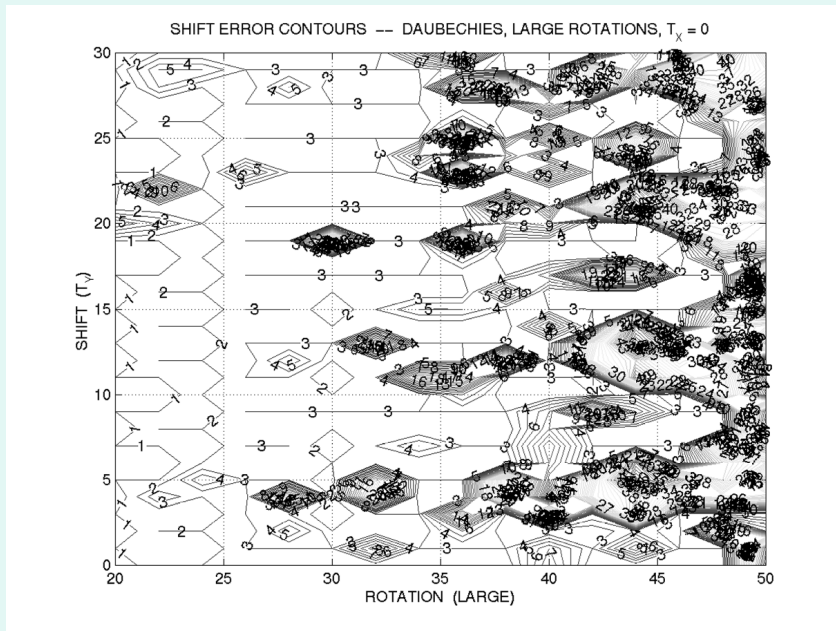
Synthetic Image Generation



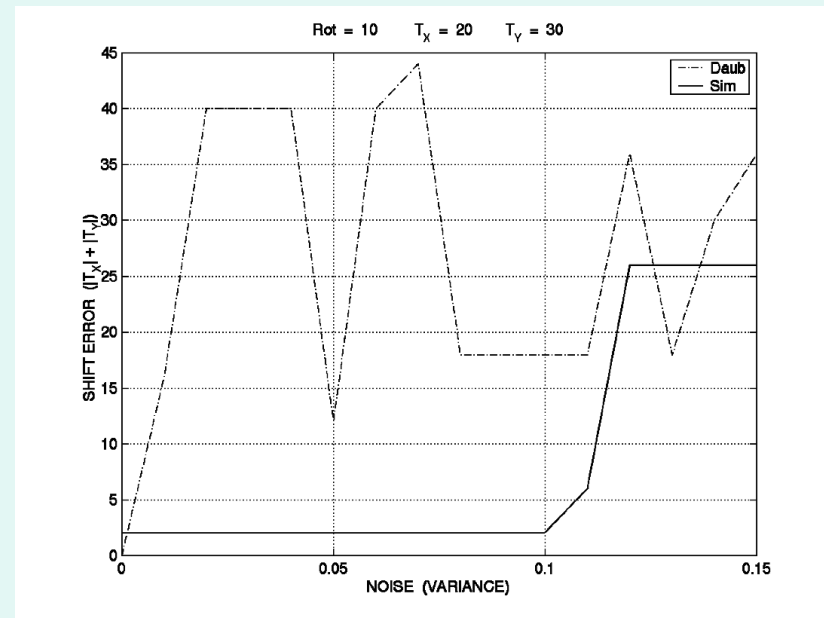
Synthetic Image Examples (Original; Warp & Noise; Warp & PSF)

Orthogonal Wavelet Studies

(Reproduced from Le Moigne & Zavorin, 2000)



Shift Errors – Daubechies – Large Rotations



*Shift Errors Function of Noise – Daubechies
Large Rotation and Translation*

Spline and Simoncelli Pyramids Studies

(Reproduced from Zavorin & Le Moigne, 2005)

	<i>Number of converged</i>	<i>Median converged error</i>	<i>Mean converged error</i>	<i>Standard deviation converged error</i>
TRU-SplC	1657/7236 \approx 22.9%	0.0219008	0.086284	0.148911
TRU-SimB	1552/7236 \approx 21.5%	0.0411122	0.141976	0.212933
TRU-SimL	3693/7236 \approx 51%	0.0214522	0.056263	0.109165

Average Error for Converged Region of Test Dataset (Warp & Noise)

	<i>Number of converged</i>	<i>Median converged error</i>	<i>Mean converged error</i>	<i>Standard deviation converged error</i>
TRU-SplC	2831/9801 \approx 28.9%	0.285565	0.300596	0.082751
TRU-SimB	725/9801 \approx 7.4%	0.052036	0.065967	0.032609
TRU-SimL	2918/9801 \approx 29.8%	0.320529	0.331067	0.091969

Average Error for Converged Region of Test Dataset (Warp & PSF)

	<i>Number of converged</i>	<i>Median converged error</i>	<i>Mean converged error</i>	<i>Standard deviation converged error</i>
TRU-SplC	1424/7236 \approx 19.7%	0.216392	0.278916	0.168494
TRU-SimB	1415/7236 \approx 19.6%	0.164233	0.252788	0.213441
TRU-SimL	4038/7236 \approx 55.8%	0.243106	0.289142	0.142683

Average Error for Converged Region of Test Dataset (Warp & PSF & Noise)

Spline and Simoncelli Pyramids Studies

(Reproduced from Zavorin & Le Moigne, 2005)

	<i>Number of converged</i>	<i>Median converged error</i>	<i>Mean converged error</i>	<i>Standard deviation converged error</i>
TRU-SplC	1657/7236 \approx 22.9%	0.0219008	0.086284	0.148911
TRU-SimB	1552/7236 \approx 21.5%	0.0411122	0.141976	0.212933
TRU-SimL	3693/7236 \approx 51%	0.0214522	0.056263	0.109165

Average Error for Converged Region of Test Dataset (Warp & Noise)

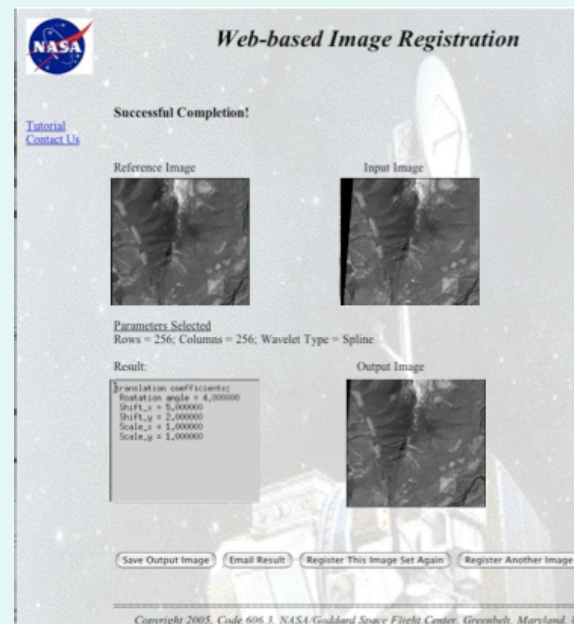
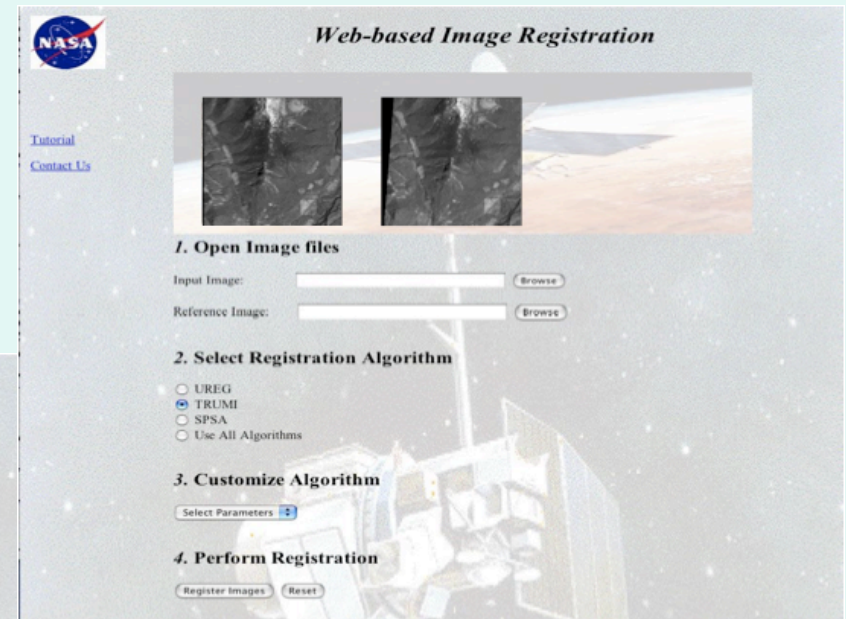
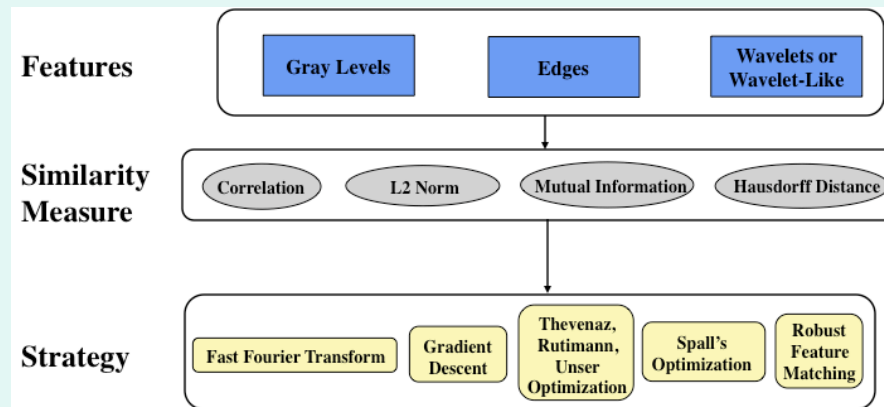
	<i>Number of converged</i>	<i>Median converged error</i>	<i>Mean converged error</i>	<i>Standard deviation converged error</i>
TRU-SplC	2831/9801 \approx 28.9%	0.285565	0.300596	0.082751
TRU-SimB	725/9801 \approx 7.4%	0.052036	0.065967	0.032609
TRU-SimL	2918/9801 \approx 29.8%	0.320529	0.331067	0.091969

Average Error for Converged Region of Test Dataset (Warp & PSF)

	<i>Number of converged</i>	<i>Median converged error</i>	<i>Mean converged error</i>	<i>Standard deviation converged error</i>
TRU-SplC	1424/7236 \approx 19.7%	0.216392	0.278916	0.168494
TRU-SimB	1415/7236 \approx 19.6%	0.164233	0.252788	0.213441
TRU-SimL	4038/7236 \approx 55.8%	0.243106	0.289142	0.142683

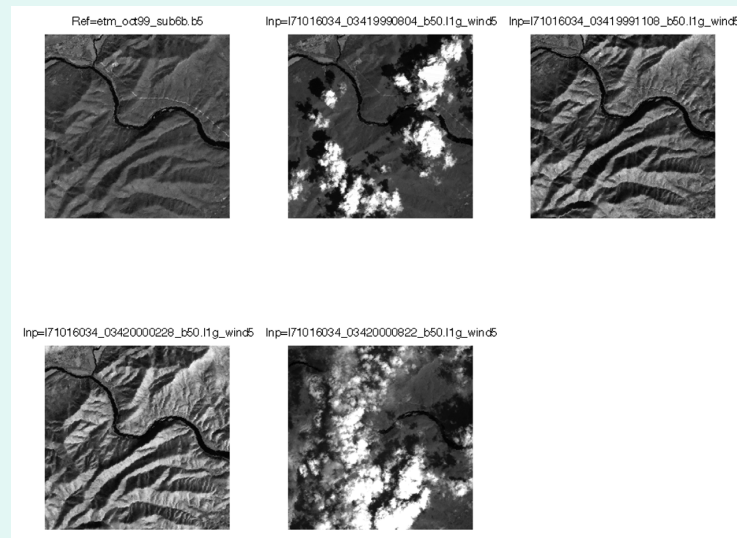
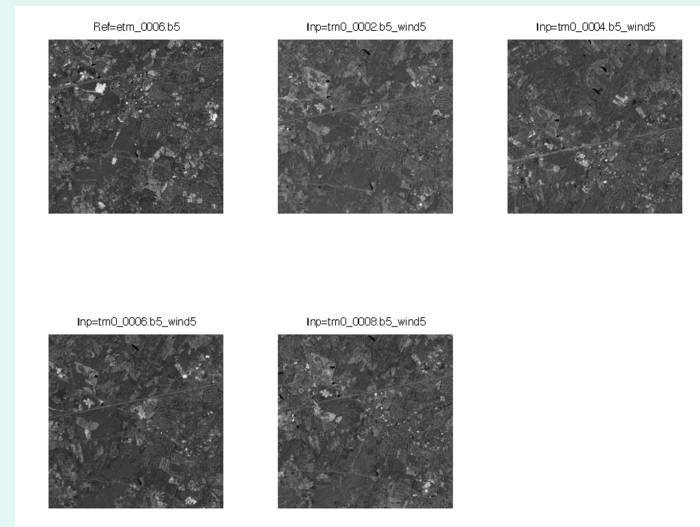
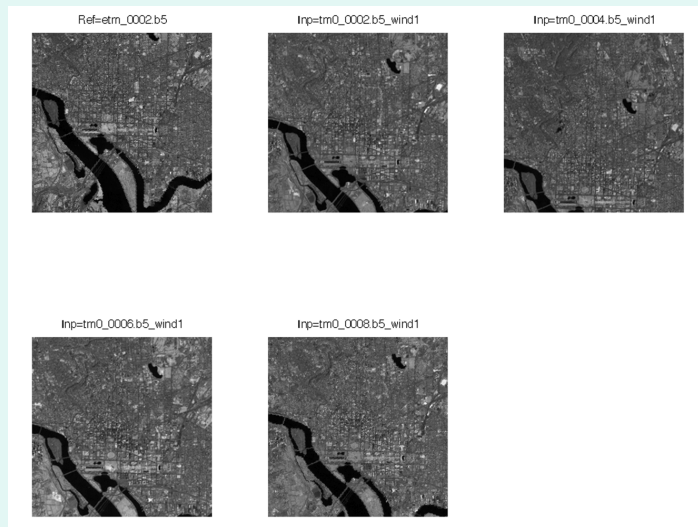
Average Error for Converged Region of Test Dataset (Warp & PSF & Noise)

A Framework for the Analysis of Various Image Registration Components



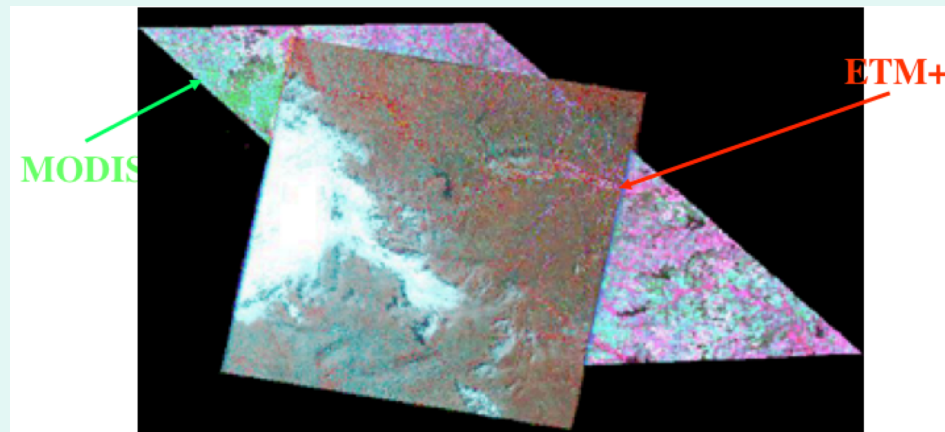
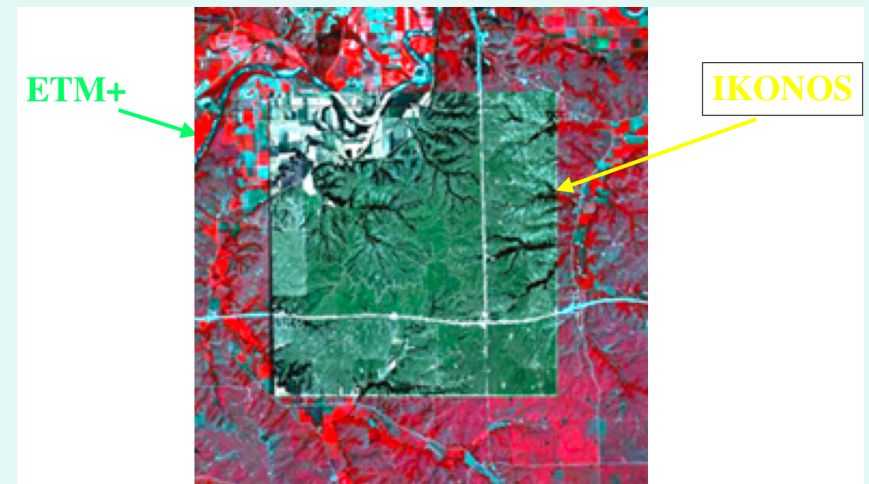
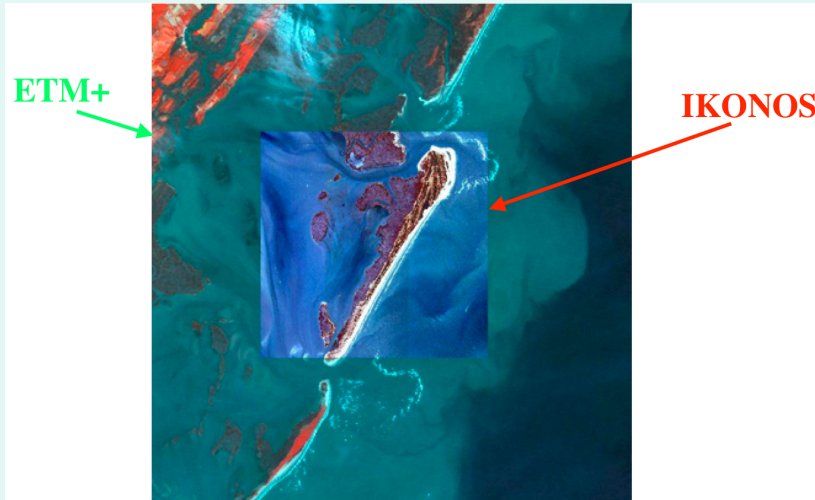
TARA (Toolbox for Automated Registration and Analysis)

Algorithm Testing Using Landsat-TM Multitemporal Data



Algorithm Testing Using Multisensor Data (ETM+, IKONOS and MODIS)

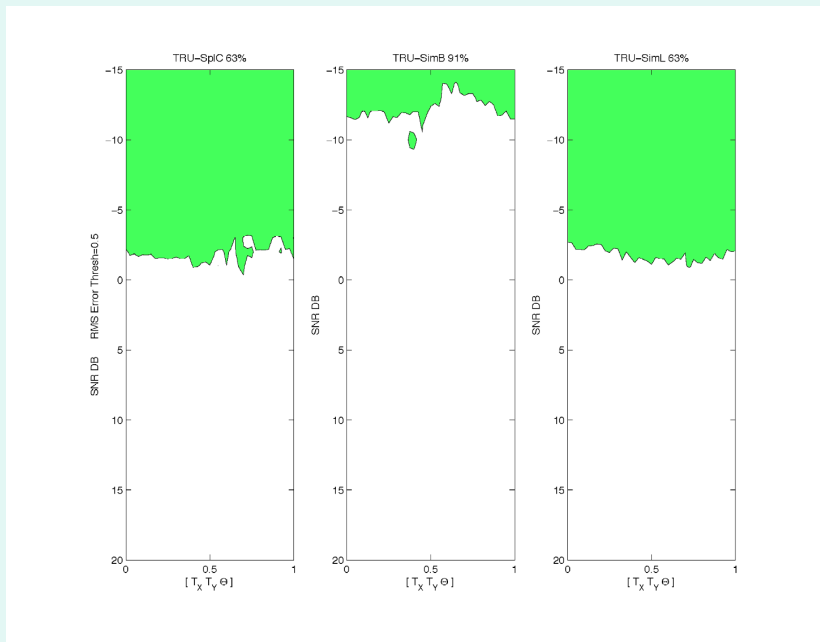
Red and NIR Bands; 30m – 4m – 250 and 500 m respectively



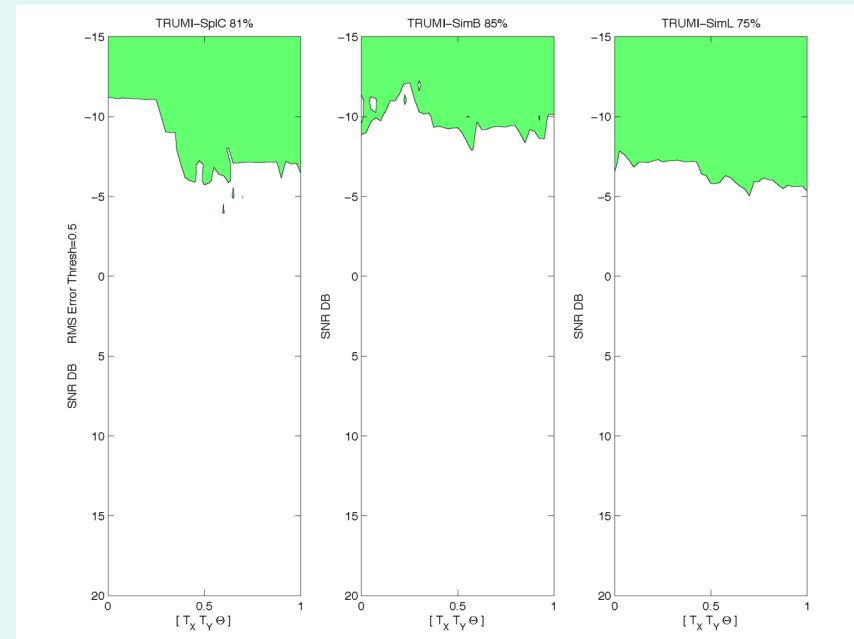
Framework Testing Using Synthetic Datasets

Marquart-Levenberg Optimization Using L2-Norm and Mutual Information

(Reproduced from Zavorin & Le Moigne, 2005)



*Contour Plot "SameRadNoisy" Dataset
Optimization Using L2-Norm
Threshold of 0.5*

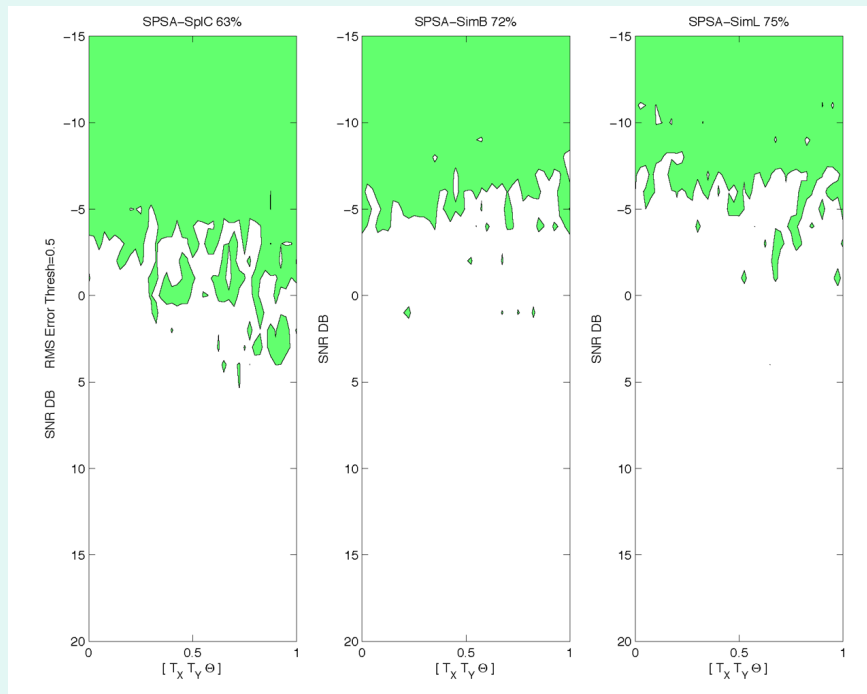


*Contour Plot "SameRadNoisy" Dataset
Optimization Using Mutual Information
Threshold of 0.5*

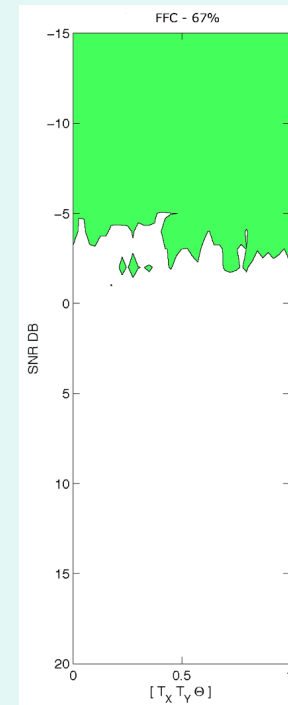
Framework Testing Using Synthetic Datasets

Stochastic Gradient Optimization Using L2-Norm and Mutual Information

(Reproduced from Zavorin & Le Moigne, 2005)



*Contour Plot "SameRadNoisy" Dataset
Stochastic Gradient and Mutual Information
Threshold of 0.5*



*Contour Plot "SameRadNoisy" Dataset
Fast Fourier Correlation
Threshold of 0.5*

Multitemporal Datasets

Robust Feature Matching Using Simoncelli Band-Pass Features

(Reproduced from Netanyahu et al, 2004)

Scene	RFM REGISTRATION			MANUAL GROUND TRUTH			ABSOLUTE ERROR		
	Q	T _x	T _y	Q	T _x	T _y	DQ	DT _x	DT _y
840827	0.031	4.72	-46.88	0.026	5.15	-46.26	0.005	0.43	0.62
870516	0.051	8.49	-45.62	0.034	8.58	-45.99	0.017	0.09	0.37
900812	0.019	17.97	-33.36	0.029	15.86	-33.51	0.010	0.11	0.15
960711	0.049	8.34	- 101.97	0.031	8.11	- 103.18	0.018	0.23	1.21

*Results of Multitemporal Registration
Using Landsat-TM Data over DC/Baltimore Area*

Scene	RFM REGISTRATION			MANUAL GROUND TRUTH			ABSOLUTE ERROR		
	Q	T _x	T _y	Q	T _x	T _y	DQ	DT _x	DT _y
990804	0.009	0.36	3.13	0.002	0.04	3.86	0.011	0.40	0.73
991108	0.000	1.00	13.00	0.002	1.20	13.53	0.002	0.20	0.53
000228	0.005	0.88	-2.32	0.008	1.26	2.44	0.003	0.38	0.12
000822	0.002	0.41	9.22	0.011	0.35	9.78	0.013	0.06	0.56

*Results of Multitemporal Registration
Using Landsat-TM Data over Virginia Area*

Multisensor Datasets

All Algorithm Comparison

(Reproduced from Le Moigne et al, 2001)

PAIR TO REGISTER	FFC		GGD		SIMB-CORRE		SIMB-MI		RFM	
	Rot	Transl	Rot	Transl	Rot	Transl	Rot	Transl	Rot	Transl
ETM_nir/ETM_red	otation =0, Translation = (0,0) computed by all methods, using 7 sub-window pair									
IKO_nir/ETM_nir	-	(2, 1)	0.0001	(1.99,-0.06)	0	(2, 0)	0	(2, 0)	0.00	(0.0, 0.0)
IKO_red/ETM_red	-	(2, 1)	-0.0015	(1.72, 0.28)	0	(2, 0)	0	(2, 0)	0.00	(0.0, 0.0)
ETM_nir/MODIS_nir	-	(-2,-4)	0.0033	(-1.78,-3.92)	0	(-2, -4)	0	(-2, -4)	0.00	(-3.0,3.5)
ETM_red/MODIS_red	-	(-2,-4)	0.0016	(1.97,-3.90)	0	(-2, -4)	0	(-2, -4)	0.00	(-2.0,-3.5)
MODIS_nir/SEAWIFS	-	(-9, 0)	0.0032	(-8.17 ,0.27)	0	(-8, 0)	0	(-9, 0)	0.50	(-6.0,2.0)
MODIS_red/SEAWIFS	-	(-9, 0)	0.0104	(-7.61, 0.57)	0	(-8, 0)	0	(-8, 0)	0.25	(-7.0,1.0)

*Results of Multisensor Registration
Using ETM, IKONOS and MODIS Data over Konza Agricultural Area*

- Similar Tests performed on:
 - Urban Area (USDA site; Greenbelt, MD)
 - Coastal Area (VA Coast)
 - Agricultural Area (Cascades Site, CO)
 - Mountainous Area (Konza Prairie, Kansas)
- Consistency studies show between 0.125 and 0.25 pixel errors using circular registrations of IKONOS NIR and Red data
- Additional studies performed on EO1-Hyperion data

Fusion of Remotely Sensed Data

- Data Fusion

- Use multi-source data of **different natures** to increase quality of information contained in data (Pohl and Genderen, 1998)
- A **process** dealing with **association, correlation, and combination** of data and information from single and **multiple** sources to achieve **refined position and identity estimates**, and complete and timely assessments of situations and threats, and their significance (Hall and Llinas, 2001).

- Image Fusion

- Data are images
- General Objectives:
 - » Image sharpening
 - » Improving registration/classification accuracy
 - » Temporal change detection
 - » Feature enhancement
- Example Application
 - » Invasive Species Forecasting System
 - » Objective
 - » **Improvement of classification accuracy**
 - » **Tamarisk, Leafy Spurge, Cheat grass, Russian olive, etc.**
 - » **Feature enhancement**

Image Fusion Methods

- Principal Component Analysis, PCA
 - Input
 - Multivariate data set of inter-correlated variables
 - Output
 - Data set of new uncorrelated linear combinations of the original variable
- Wavelet-based Fusion
 - Use of Different Subbands in Reconstruction
- Cokriging

Image Fusion Methods

Wavelet-Based Image Fusion

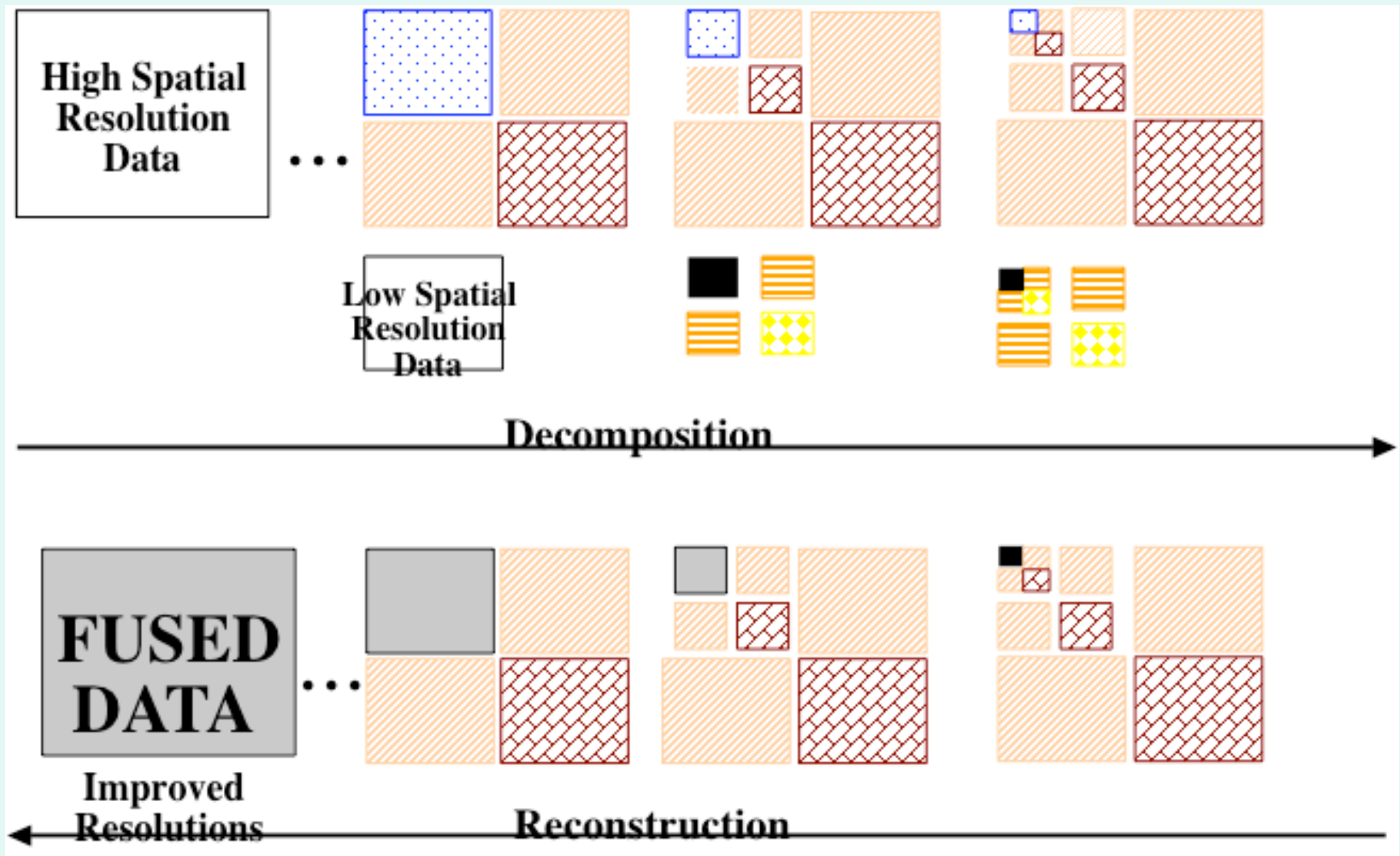


Image Fusion Methods

Cokriging

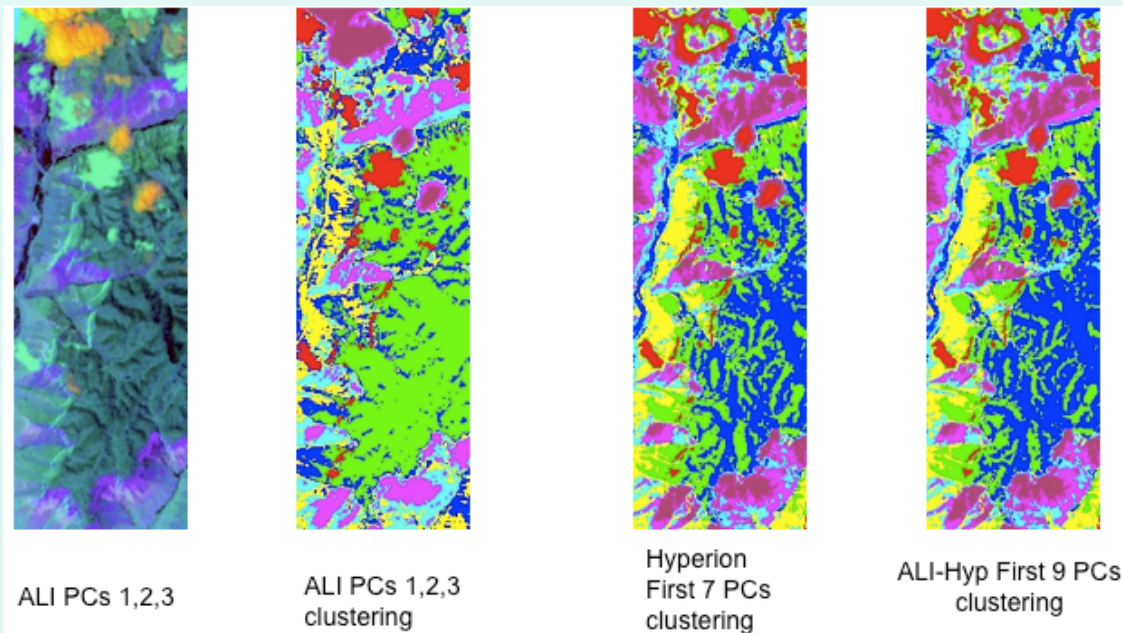
- Interpolation Method
 - Geo-statistics, mining, and petroleum engineering applications (pioneered by Danie Krige, 1951)
 - Generalized version of *kriging (B.L.U.E)*:
 - *Best*: aims to minimize variance of the errors
 - *Linear*: estimates are weighted linear combination of the available data
 - *Unbiased*: tries to have mean residual, or error, equal to zero.
 - *Estimator*
- Interpolation using more than one type of variable to estimate an unknown value at a particular location
- Goal of cokriging is to *minimize variance of error* subject to some constraints (to ensure unbiasedness of our estimate)

Image Fusion Experiments

Using Principal Component Analysis

(Reproduced from Memarsadeghi et al, 2005)

- Input
 - 9 bands of ALI
 - 140 bands of Hyperion (calibrated and not corrupted bands)
 - Stack of both ALI and Hyperion bands above
- Output
 - Same number of PCs as input bands
 - Select PCs containing 99% of information



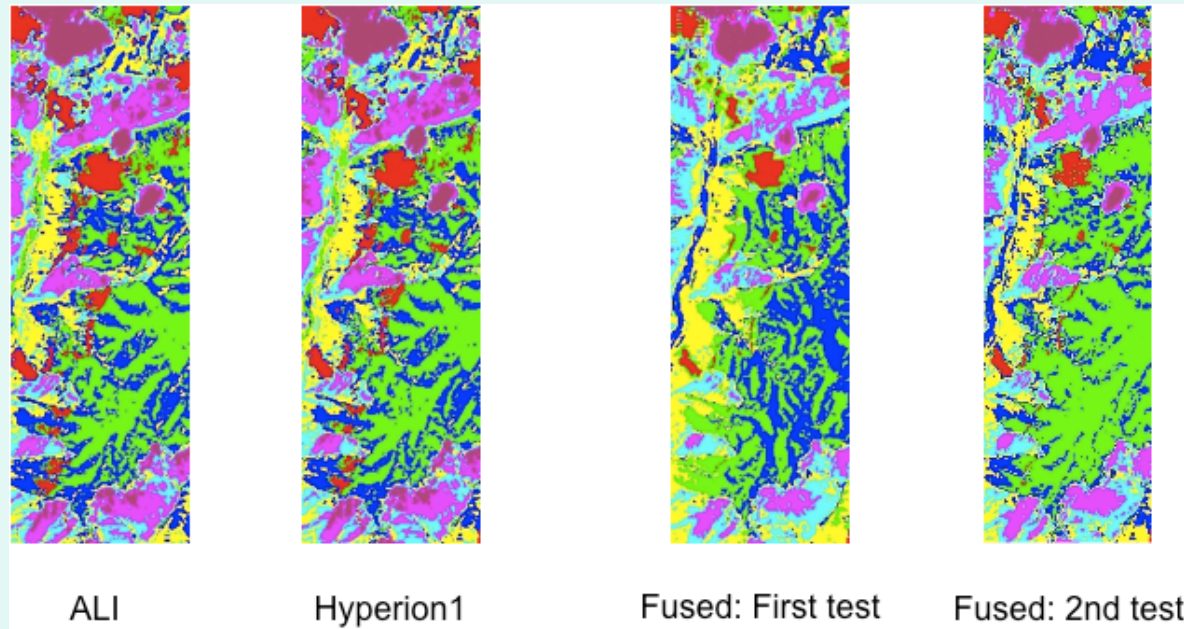
ALI V	Hyp V	Fused V
143.98	137.64	180.10

Image Fusion Experiments

Using Wavelet-Based Fusion

(Reproduced from Memarsadeghi et al, 2005)

- Fuse each multispectral band of ALI with one band of Hyperion
 - For each of 9 ALI bands
 - Select a Hyperion band within the wavelength range of corresponding ALI band which is
 - » closest to the center of ALI's wavelength range (experiment 1)
 - » least correlated to the corresponding ALI band (experiment 2)
 - Clustering of fusion result of 9 bands of ALI with 9 bands of Hyperion
 - Fusion: 4 Levels of Decomposition, Daubechies Filter of size 2

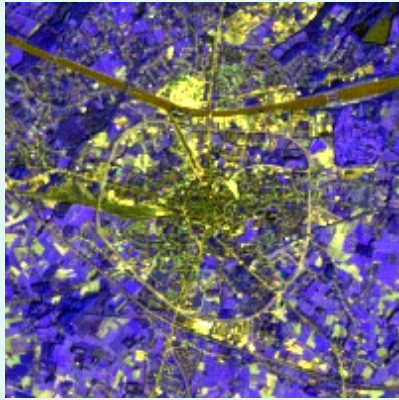


- Experiment 1 Variances: ALI: 179.73; Hyperion: 159.96; Fused: 195.27
- Experiment 2 Variances: ALI: 179.73; Hyperion: 165.34; Fused: 173.77

Image Fusion Experiments

Using Cokriging

(Reproduced from Memarsadeghi et al, 2006)



Landsat-TM
Multispectral Bands 2, 3, 4
(30m resolution)



Landsat-TM Panchromatic
(15m resolution)

Image Fusion Experiments

Using Cokriging (cont.)

(Reproduced from Memarsadeghi et al, 2006)

*Landsat-7 Multispectral
Bands 2,3 and 4*



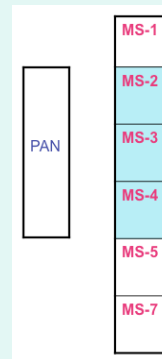
Landsat-7 Panchromatic Band 8



FUSION

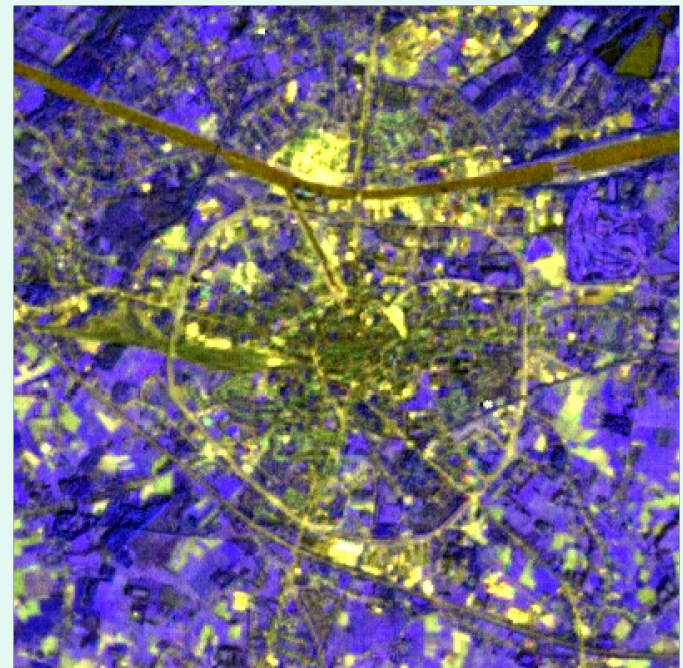
Pan + MS-2	⇒	fused_b2
Pan + MS-3	⇒	fused_b3
Pan + MS-4	⇒	fused_b4

**Spectral Resolution
1 pixel of an MS band**



x1	y1	p1	?
x2	y2	p2	?
x3	y3	p3	ms1
x4	y4	p4	?

*Landsat-7 Pan-Sharpened MS Bands 2,3 and 4
Through Cokriging with Pan Band 8*



Results:

- Correlation: Wavelet: 0.86; PCA: 0.91; Cokriging: 0.92
- Entropy: Wavelet: 3.44; PCA: 3.87; Cokriging: 3.92

References

Jacqueline Le Moigne

- A. Cole-Rhodes, K. Johnson, J. Le Moigne, and I. Zavorin, 2003, "Multiresolution Registration of Remote Sensing Imagery by Optimization of Mutual Information Using a Stochastic Gradient," *IEEE Transactions on Image Processing*, Vol. 12, No. 12, pp. 1495-1511, December 2003.
- J. Le Moigne, N. Netanyahu, and N. Laporte, 2001, "Enhancement of Tropical Land Cover Mapping with Wavelet-Based Fusion and Unsupervised Clustering of SAR and Landsat Image Data," Proceedings of the 8-th SPIE International Symposium on Remote Sensing, Image and Signal Processing for Remote Sensing VII, Vol. #4541, Toulouse, France, September 17-21, 2001.
- J. Le Moigne, W.J. Campbell, and R.F. Crompt, 2002, "An Automated Parallel Image Registration Technique of Multiple Source Remote Sensing Data," *IEEE Transactions on Geoscience and Remote Sensing*, Vol. 40, No. 8, pp. 1849-1864, August 2002.
- J. Le Moigne and R. Eastman, 2005, "Multi-Sensor Registration for Earth Remotely Sensed Imagery," *published in* R.S. Blum and Z. Liu (eds), *Multi-Sensor Image Fusion and its Application*, Marcel Dekker & CRC Press Publication.
- J. Le Moigne, N. Netanyahu, and R. Eastman, 2010, *Registration for Earth Remote Sensing*, Cambridge University Press, in press (available November 2010).
- N. Memarsadeghi, J. Le Moigne, D. Mount, and J. Morissette, 2005, "A New Approach to Image Fusion Based on Cokriging," FUSION'2005, 8th International Conference on Information Fusion, Philadelphia, Pennsylvania, July 25-28, 2005, Volume 1, pages 622-629.
- N. Memarsadeghi, J. Le Moigne, and D. Mount, 2006, "Image Fusion Using Cokriging," 2006 IEEE International Geoscience and Remote Sensing Symposium, IGARSS'06, Denver, CO, July 2006.
- N. Netanyahu, J. Le Moigne and J. Masek, 2004, "Geo-Registration of Landsat Data by Robust Matching of Wavelet Features," *IEEE Transactions on Geoscience and Remote Sensing*, Volume 42, No. 7, pp. 1586-1600, July 2004.
- H.S. Stone, J. Le Moigne, and M. McGuire, 1999, "Image Registration Using Wavelet Techniques," *IEEE Transactions on Pattern Analysis and Machine Intelligence, PAMI*, Vol. 21, No.10, October 1999.
- I. Zavorin, and J. Le Moigne, 2005, "On the Use of Wavelets for Image Registration," *IEEE Transactions on Image Processing*, Vol. 14, No. 6, June 2005.

ACRONYMS

- AVHRR: Advanced Very High Resolution Radiometer
- CP or GCP: Control Point or Ground Control Point
- GSHHS: Global Self-consistent Hierarchical High-resolution Shoreline
- GOES: Geostationary Operational Environmental Satellite
- GSFC: Goddard Space Flight Center
- MISR: Multiangle Imaging SpectroRadiometer
- MODIS: MODerate resolution Imaging Spectrometer
- NDVI: Normalized Difference Vegetation Index
- SeaWiFS: Sea-viewing Wide Field-of-view Sensor
- SPOT: Satellite Pour l'Observation de la Terre
- WSU: Wright State University